

## CHAPTER IV

### RESULTS AND DISCUSSION

#### 4.1 Molecular Weight Characterization

Molecular weights of PS680A, PI, PE5200B and PVAc500 were characterized by three instruments: Ubbelohde Viscometer, Gel Permeation Chromatography (GPC) and Cone and Plate Rheometer. Table 4.1 shows the molecular weight of each homopolymer. The average molecular weights of homopolymers are close to the values quoted from the company as shown in Table 3.1.

**Table 4.1** The molecular weight of homopolymer characterized by Ubbelohde Viscometer and GPC

Polymer	Source	$M_w^{\#}$ (g/mole)	$M_w^*$ (g/mole)	$\bar{M}_v^{**}$	$M_n^*$ (g/mole)
PS680A	Dow Chemical	-	$1.87 \cdot 10^5$	$1.99 \cdot 10^5$	$5.72 \cdot 10^4$
PI	Japan Synthetic Rubber	$1.00 \cdot 10^6$	$1.03 \cdot 10^6$	$1.05 \cdot 10^6$	$6.47 \cdot 10^4$
HDPE5200B	BPE	-	$7.60 \cdot 10^5$	-	$5.02 \cdot 10^4$
SIS bcp	Shell Chemical Company	-	$7.47 \cdot 10^4$	-	-
PVAc500	Aldrich	$5.00 \cdot 10^5$	$5.79 \cdot 10^5$	$5.40 \cdot 10^5$	$7.91 \cdot 10^4$

# quoted from company

\* From GPC

\*\* From Ubbelohde Viscometer

#### 4.1.1 Viscosity Average Molecular Weight ( $\overline{M}_v$ )

Molecular weight measurement by the Ubbelohde viscometer is based on the viscosity parameters: the kinematic viscosity ( $\nu$ ), the dynamic viscosity ( $\eta$ ) and the intrinsic viscosity  $[\eta]$  for a given polymer - solvent system. It was determined by using the Mark-Houwink-Sakurada equation:

$$[\eta] = K\overline{M}_v^a \quad (4.1)$$

where K and a values are constant for a given polymer, solvent at a particular temperature. All parameters used in calculating  $\overline{M}_v$  of the homopolymers are listed in Table 4.2.

**Table 4.2** Mark-Houwink-Sakurada parameters for each homopolymer (Brandrup and Immergut, 1989)

Polymers	solvent*	Ubbelohde Viscometer size	Calibration Constant (k)	Temperature <sup>#</sup> (°C)	K (*10 <sup>-3</sup> ) <sup>#</sup> (ml/g)	a <sup>#</sup>
PS	Toluene	25	0.00203	25	13.4	0.71
PVAc	chloroform	25	0.00203	25	20.3	0.72
PI	toluene	50	0.00407	30	20	0.728

<sup>#</sup>reference

From the plots of  $\eta_{sp}/C$  and  $\ln(\eta_r)/C$  versus concentration, the intrinsic viscosity was determined from Y-intercept of this graph (Appendix A1). The intrinsic viscosity of PS680A, PVAc500 and PI are 77.76, 272.3 and 485.28 cc/g, respectively, as illustrated in figure 4.1(a-c). So the corresponding molecular weights ( $\overline{M}_v$ ) of the homopolymers are  $1.99 \times 10^5$ ,  $5.40 \times 10^5$  and  $1.05 \times 10^5$  g/mole, respectively.

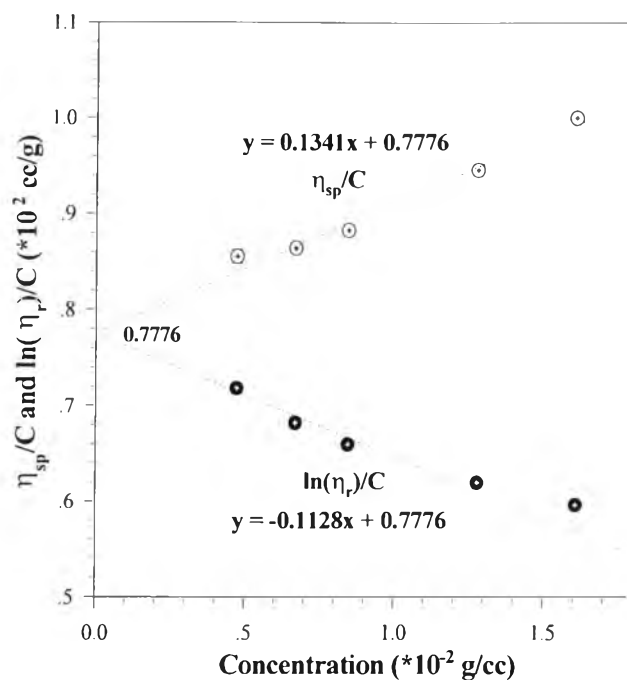


**Figure 4.1a** Schematic of plot between  $\eta_{sp}/C$  and  $\ln(\eta_r)/C$  versus  $C$  of PS680A at 25°C. The extrapolation to zero concentration is  $[\eta]$ .

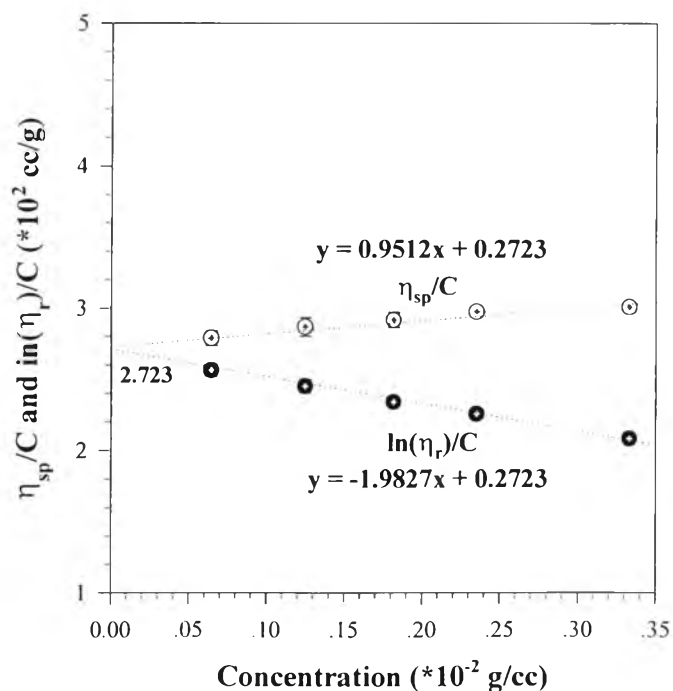


**Figure 4.1b** Schematic of plot between  $\eta_{sp}/C$  and  $\ln(\eta_r)/C$  versus  $C$  of PVAc500 at 25°C. The extrapolation to zero concentration is  $[\eta]$ .

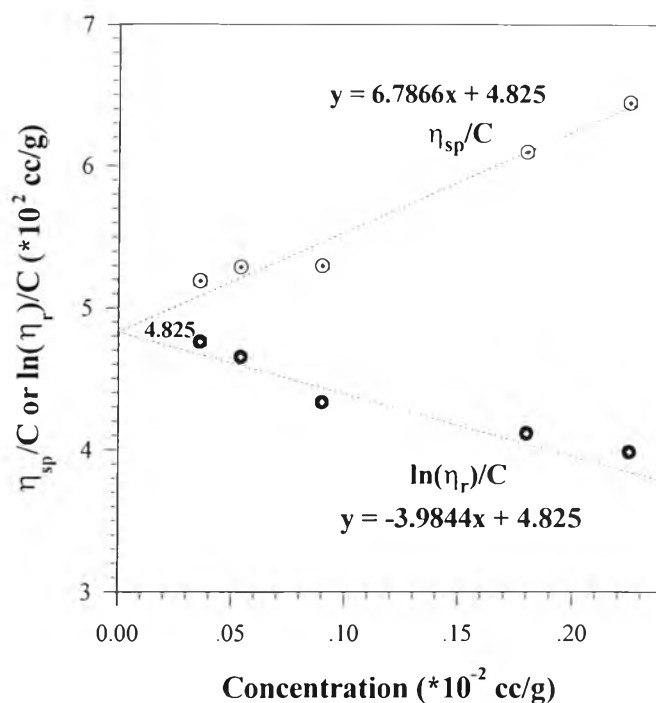


**Figure 4.1c** Schematic of plot between  $\eta_{sp}/C$  and  $\ln(\eta_r)/C$  versus  $C$  of PI at 30°C. The extrapolation to zero concentration is  $[\eta]$ .

## 4.2 Rheological Characterizations

Two rheological properties, the shear viscosity and the first normal stress difference ( $N_1$ ), were measured by using a 25-mm cone and plate rheometer in the steady state testing mode as a function of shear rate from 10 to 200 s<sup>-1</sup>.

### 4.2.1 The Shear Viscosity ( $\eta$ )

The shear viscosity is traditionally regarded as the most important rheological property and any practical study requiring a knowledge of material response would automatically turn to the viscosity in the first instance. It was measured as a function of shear rate at 220°C by using a 25-mm cone and plate rheometer. The results are shown in figure 4.2a to 4.2c. The shear

viscosity decreases with increasing the shear rate indicating that all of them exhibit the shear-thinning behavior. The viscosity of PI minor phase in the three polymer pairs systems, PS680A/PI, PVAc500/PI and PE5200B/PI, are lower than that of the matrix in the shear rate range of 10 to 200  $\text{s}^{-1}$ .

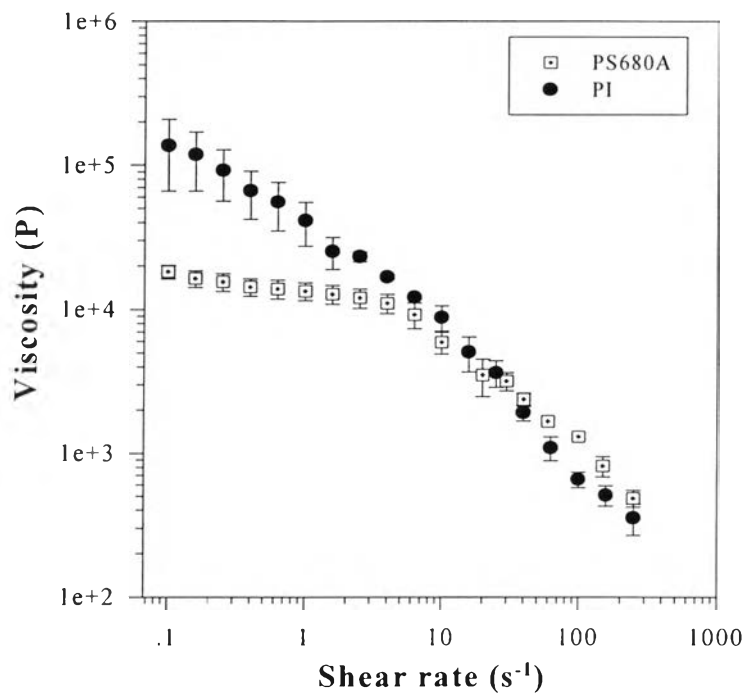


**Figure 4.2a** The shear viscosities of PS680A and PI as a function of shear rate at 220°C.

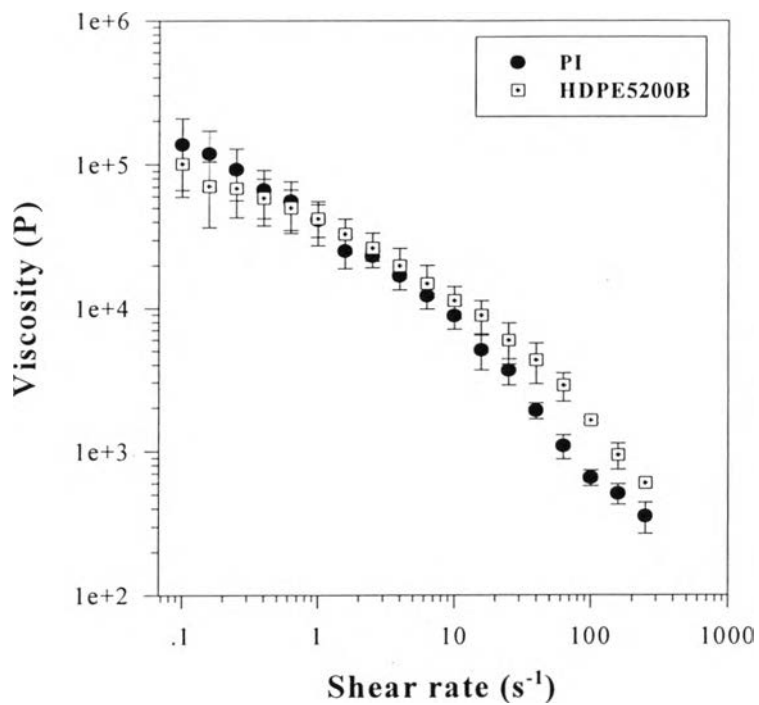


**Figure 4.2b** The shear viscosities of PE5200B and PI as a function of shear rate at 220°C.

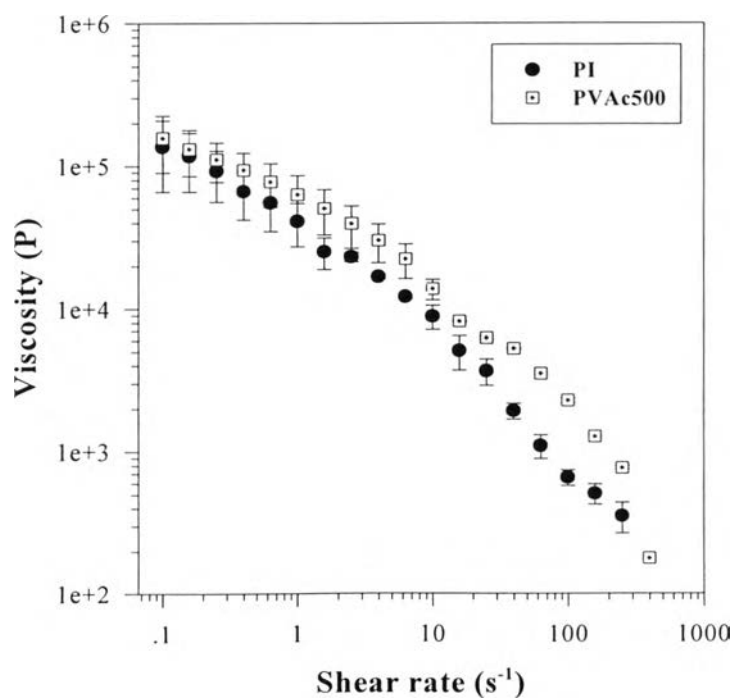


**Figure 4.2c** The shear viscosities of PVAc500 and PI as a function of shear rate at 220°C.

The zero shear viscosity can be measured by extrapolating the shear viscosity toward the zero shear rates. The results are summarized in Table 4.3. The zero shear viscosity of HDPE5200B, PVAc500 and PI have nearly the same values, which are around  $10^5$  Poise whereas PS680A has the lowest value.

**Table 4.3** The zero shear viscosity,  $\eta_0$ , of homopolymers at 220°C

Homopolymers	Zero shear viscosity (P)
HDPE5200B	$(1.01 \pm 0.41) * 10^5$
PS680A	$(1.83 \pm 0.20) * 10^4$
PVAc500	$(1.57 \pm 0.68) * 10^5$
PI	$(1.37 \pm 0.71) * 10^5$

#### 4.2.2 The First Normal Stress Difference ( $N_1$ )

The first normal stress difference ( $N_1$ ), generally, is a positive function of the shear rate and may have a power-law behavior over a range of shear rates (Barnes *et al.*, 1989). It was measured in the same procedure as of the shear viscosity measurement and results of all polymers at 220°C are shown in figure 4.3a to 4.3c. The first normal stress difference ( $N_1$ ) for each polymer increases with increasing shear rate. For PS680A/PI and HDPE5200B/PI blends, the first normal stress difference of PI minor phase is always smaller than that of the matrix along the same range of shear rates whereas the values for PVAc500 and PI are close to each other at any shear rates.

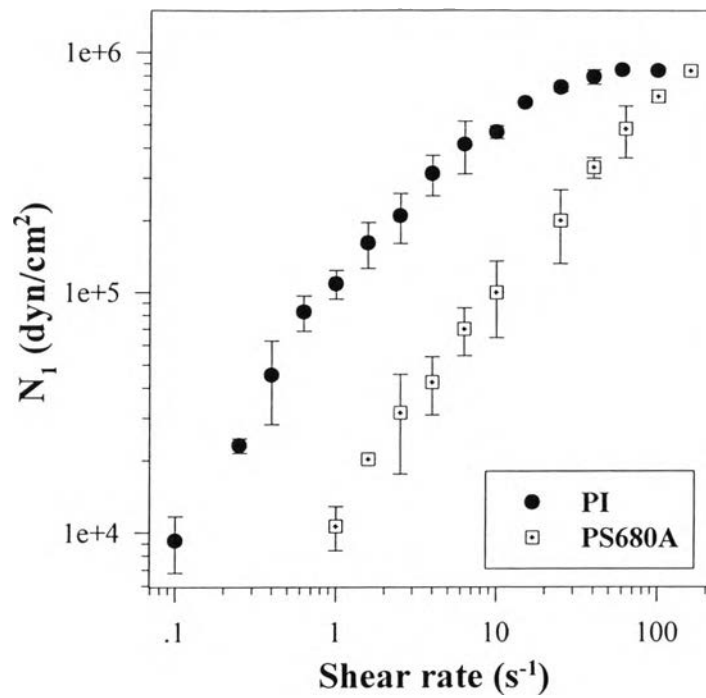


**Figure 4.3a** The first normal stress difference of PS680A and PI as a function of shear rate at 220°C.

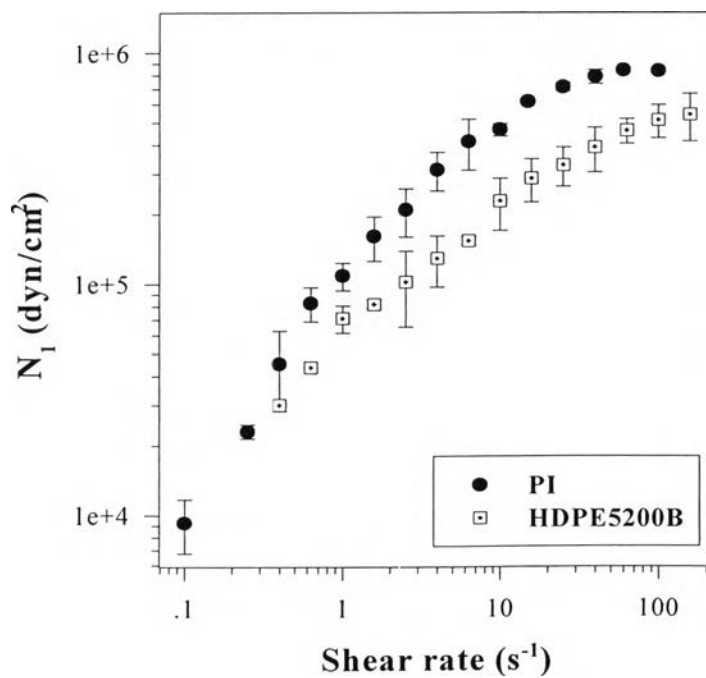


**Figure 4.3b** The first normal stress difference of HDPE5200B and PI as a function of shear rate at 220°C.



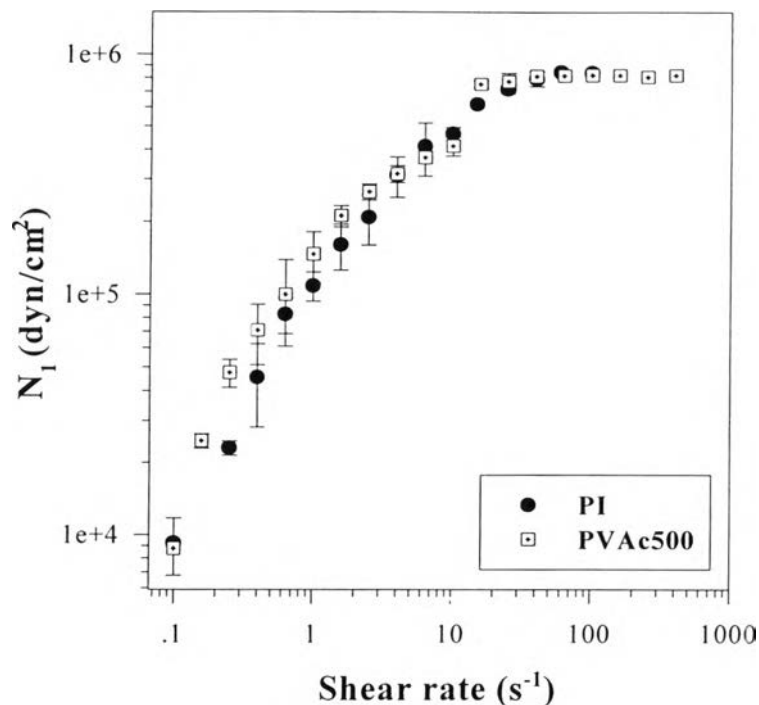


**Figure 4.3c** The first normal stress difference of PVAc500 and PI as a function of shear rate at 220°C.

The first normal stress difference generally increases with increasing shear rate. The results show that the plateau curve is obtained at high shear rate. This is because the maximum  $N_1$  for the 25-mm diameter of cone and plate fixture is  $1.00 \times 10^6$  dyn/cm<sup>2</sup>.

#### 4.2.3 The Viscosity Ratio and Normal Stress Difference Ratio of Polymer Blends

Several basic parameters are important in controlling particle deformation: blend's composition (Cigana, Favis and Jerome, 1996), elasticity ratio (Levitt and Macosko, 1996), viscosity ratio (Favis and Chalifoux, 1987) and so on.

a) *The shear viscosity ratio ( $\eta_r$ )*

The viscosity ratio of the polymer blends is defined as the ratio of dispersed phase's viscosity ( $\eta_d$ ) over the matrix phase's viscosity ( $\eta_m$ ). The viscosity ratio of each polymer blend was determined by measuring the shear viscosity of each phase as a function of shear rate, as shown in figure 4.2a to 4.2c. It turns out that the viscosity ratio is also a function of shear rate as illustrated in figure 4.4. For PS680A/PI blend, the shear viscosity ratio is varied dramatically between 1.43 to 7.49 within the shear rate of 0.1 to 20  $s^{-1}$  and it is quite different from the other two polymer systems, HDPE5200B/PI and PVAc500/PI blends which provide the values between 0.58 and 1.25. At the shear rates between 20 and 200  $s^{-1}$ , the values of three polymer systems at any shear rates are close to each other and vary slightly.

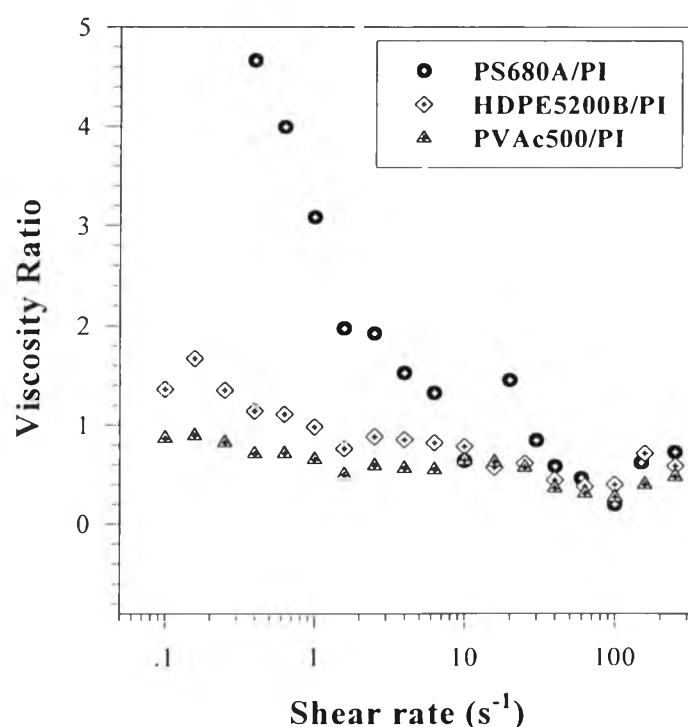


**Figure 4.4** The shear viscosity ratio of three polymer blends, PS680A/PI, PVAc500/PI and HDPE5200B/PI, as a function of shear rate at 220°C.

b) *The First Normal Stress Difference Ratio ( $N_d/N_m$ )*

This parameter was also measured as a function of shear rate as shown in figure 4.5. They were obtained from the first normal stress difference of each phase, which was measured individually as a function of shear rate. The result shows that the first normal stress difference ratios of the three polymer blends vary with the shear rate and are quite different from each other especially these of PS680A/PI. At the shear rates between 0.1 and 40  $s^{-1}$ , the first normal stress difference ratio of PS680A/PI system has the highest values whereas that of PVAc500/PI at any shear rates shows the lowest values.

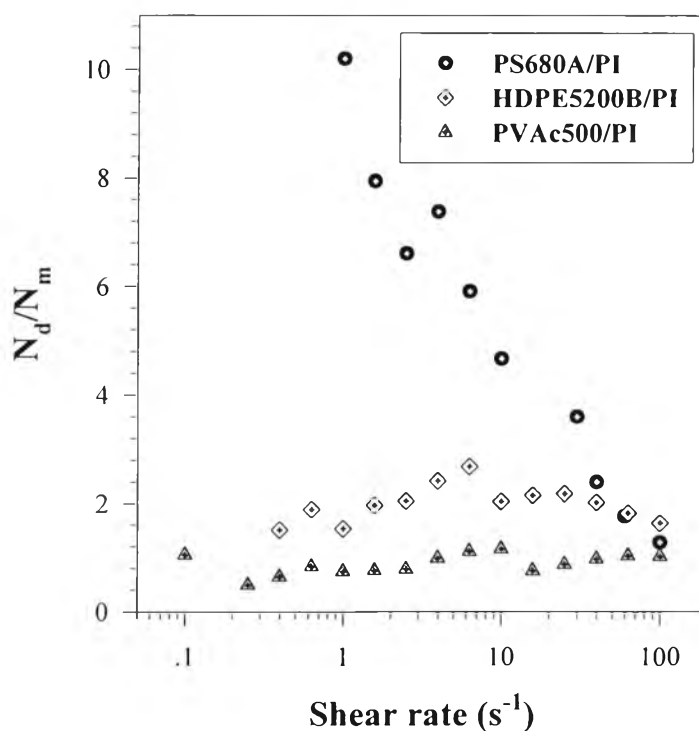


**Figure 4.5** The first normal stress difference ratio ( $N_d/N_m$ ) versus shear rate of three polymer blends, PS680A/PI, PVAc500/PI and HDPE5200B/PI, at 220°C.

### 4.3 The Effect of Mixing Time on the Morphology

The morphology of immiscible polymer blends can change with time during mixing in a twin screw extruder or a batch mixer (Wensheng and Jiasong, 1996). The equilibrium morphology with monomodal distribution can be obtained after a sufficient mixing time for a given shear rate.

The evolving morphology was determined in the terms of number average drop size ( $D_n$ ) of the minor phase versus the mixing time at the mixing shear rate of  $10 \text{ s}^{-1}$ . The mixing time was varied between 100 to 1,500 seconds in all polymer blends. The number average drop size ( $D_n$ ) was calculated as followed:

$$D_n = \frac{\sum_{i=1}^x n_i D_i}{\sum_{i=1}^x n_i} \quad (4.2)$$

where  $n$  is the number of each drop size and  $D$  is the droplet size of the PI minor phase.

#### 4.3.1) Mixing Time of Three Polymer Blends

The mixing time leading to the equilibrium morphology at  $10 \text{ s}^{-1}$  and at  $220^\circ\text{C}$  of HDPE/PI, PS/PI and PVAc/PI was investigated by a plot between the number average drop size ( $D_n$ ) versus strain unit, the product of mixing time multiplied by the shear rate, as shown in figure 4.6. For low mixing times between 100 to 500 seconds, the drop diameter of PI minor phase in the HDPE/PI blend decreases with increasing the mixing time, followed by the levelling off to a plateau value up to the mixing time of 1500 seconds. This indicates that the equilibrium morphology on the ensemble mean basis was attained at about 600 seconds at the shear rate of  $10 \text{ s}^{-1}$ . For the other two

systems, PS/PI and PVAc/PI, were also determined by the same procedure as in HDPE/PI blend. The mixing time for PS/PI and PVAc/PI are 600 and 500 seconds, respectively. It means that the equilibrium strain unit of HDPE/PI, PS/PI and PVAc/PI are 6000, 5000 and 6000, respectively. The micrographs obtained from the optical microscope for three blends are shown in Appendix C.

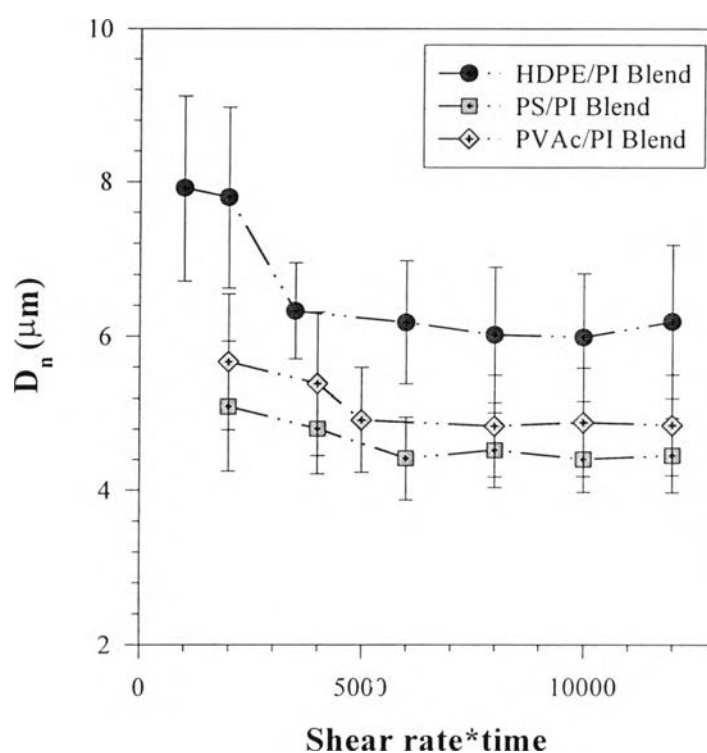


**Figure 4.6** The number average drop size ( $D_n$ ) of three polymer blends versus strain unit at the shear rate of  $10 \text{ s}^{-1}$  and at  $220^\circ\text{C}$ .

To understand more clearly, the plot between the number averaged diameter of PI minor phase in each system over its equilibrium diameter versus strain unit is shown in figure 4.7. The equilibrium morphology on the ensemble mean basis for HDPE/PI and PVAc/PI were attained when the product of mixing time multiplied by the shear rate exceeds 6,000 units whereas the values of PS/PI was obtained at the strain unit of 5,000 units.

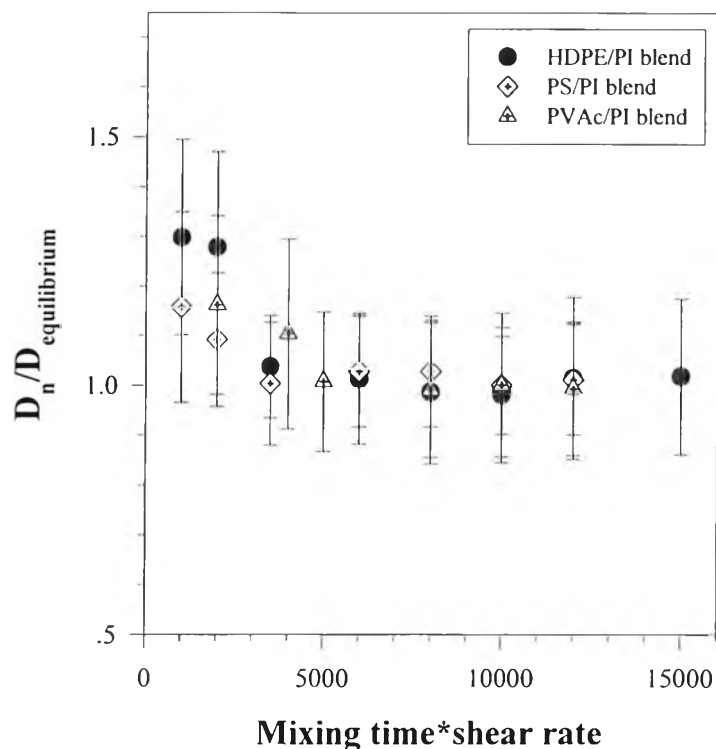


**Figure 4.7** The plot of  $D_n/D_{n\text{equilibrium}}$  versus  $(\gamma \times t)$  of HDPE5200B/PI, PS680A/PI and PVAc500/PI at the shear rate of  $10 \text{ s}^{-1}$  and at  $220^\circ\text{C}$ .

#### 4.3.2) Steady-State Drop Size Distribution at Various Mixing Time

To investigate the morphology change with mixing time at any shear rates, the average drop sizes do not have sufficient details or mechanisms involved. So the size distribution functions were determined. The distribution at various mixing time of HDPE/PI, PS/PI and PVAc/PI blends are shown in figure 4.8, 4.9 and 4.10, respectively. The distributions of droplet sizes (shown in Appendix D) change with time. The drop size distribution shifts to the lower size for longer mixing time and the monomodal distribution was obtained after a sufficient time beyond which the distribution functions did not change. So the mixing time of 600 seconds, strain unit equal to 6000, was chosen for mixing HDPE5200B/PI, PS/PI and PVAc/PI at the shear rate of  $10 \text{ s}^{-1}$  and at  $220^\circ\text{C}$ .

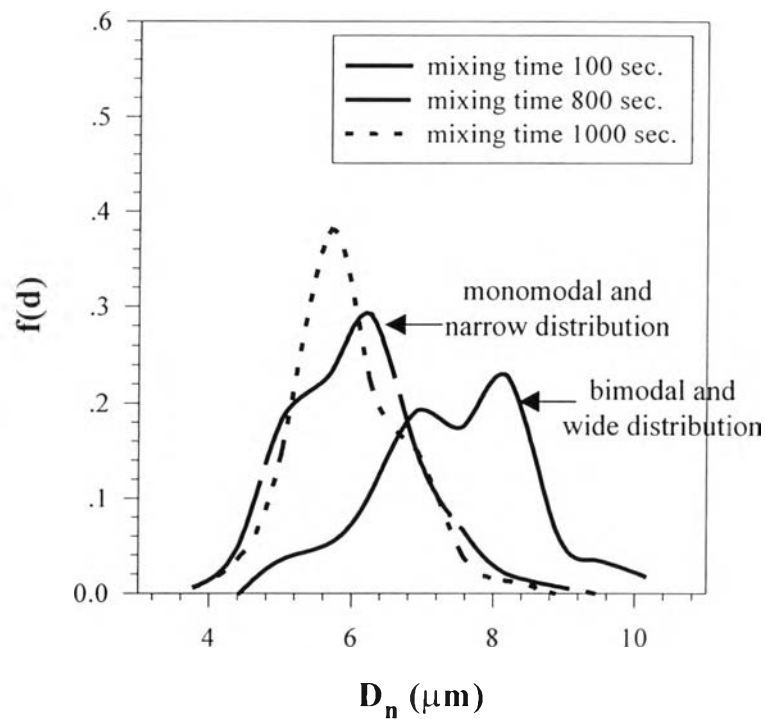


**Figure 4.8** The drop size distribution function of HDPE5200B/PI blend as a function of mixing time at  $10 \text{ s}^{-1}$ ,  $220^\circ\text{C}$ .

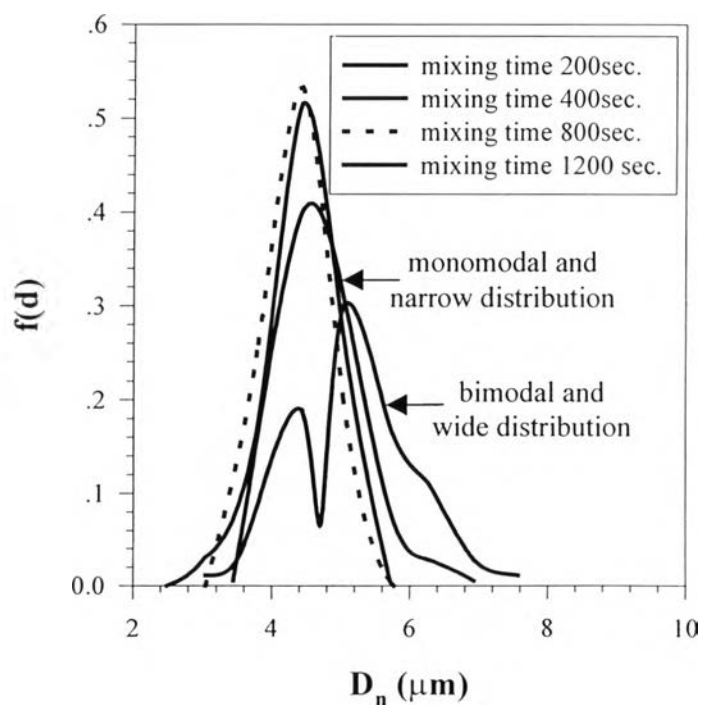


**Figure 4.9** The drop size distribution function of PS680A/PI blend as a function of mixing time at  $10 \text{ s}^{-1}$ ,  $220^\circ\text{C}$ .

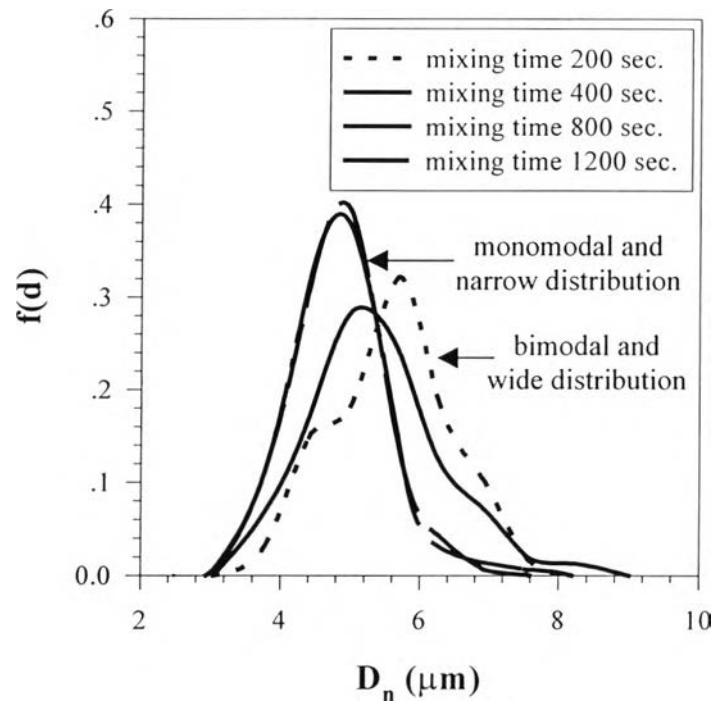


**Figure 4.10** The drop size distribution function of PVAc500/PI blend as a function of mixing time at  $10 \text{ s}^{-1}$ ,  $220^\circ\text{C}$ .

#### 4.4 Effect of Shear Rate on the Morphology

##### 4.4.1) The Equilibrium Drop Size

The shear rate is an important parameter for controlling the morphology of blends, which was studied in many research workers (Sundararaj and Macosko, 1995, Wu, 1987 and Chalivoux and Favis, 1987). Breakup behavior is commonly generated at a high shear rate whereas coalescence behavior can occur at a lower shear rate.

In this work, the effect of shear rate on equilibrium droplet size of PI minor phase in three polymer blends was investigated at shear rates between 10 and  $200 \text{ s}^{-1}$ , as shown in figure 4.11.



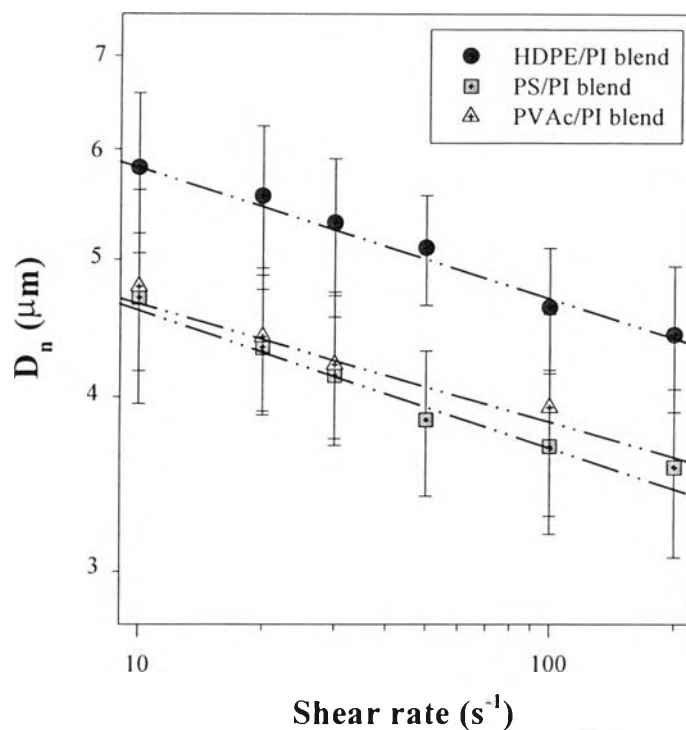


**Figure 4.11** The droplet size of PI minor phase as a function of shear rate of the HDPE5200B/PI blend, the PS680A/PI blend and the PVAc500/PI blend at 220°C. The scaling exponents of  $D_n$  versus  $\dot{\gamma}$  are -1.12, -0.90 and -0.83, respectively.

HDPE5200B/PI blend gave the largest droplet size at any shear rates while the smallest size was formed in PS680A/PI blend. In the addition, the maximum droplet size were formed at the shear rate of  $10 s^{-1}$  whereas the particle size actually decreased at higher shear rate and reached the minimum size at  $200 s^{-1}$ . The same results occurred for all polymer blends.

The PI droplet size at shear rate between  $10$  and  $200 s^{-1}$  of the three polymer blends was shown in Table 4.4 consisting of the average equilibrium droplet size, standard deviations (S.D.), the maximum drop size, and the minimum drop size.

**Table 4.4** The drop size as a function of shear rate in HDPE5200B/PI, PS680A/PI and PVAc500/PI at 220°C

Shear rate (s <sup>-1</sup> )		10	20	30	50	100	200
HDPE5200B/PI	D <sub>n</sub> (μm)	5.60	5.54	5.30	5.10	4.62	4.42
	S.D.	0.75	0.66	0.60	0.46	0.47	0.52
	Max.	7.57	7.57	7.57	6.27	5.71	5.71
	Min.	3.80	4.43	4.43	4.43	3.80	3.05
PS680A/PI	D <sub>n</sub> (μm)	4.69	4.33	4.14	3.85	3.68	3.36
	S.D.	0.52	0.42	0.41	0.45	0.49	0.46
	Max.	6.27	5.03	5.03	5.03	5.03	5.03
	Min.	3.05	3.05	3.05	2.49	3.05	2.49
PVAc500/PI	D <sub>n</sub> (μm)	4.83	4.41	4.21	-	3.93	3.83
	S.D.	0.66	0.52	0.52	-	0.64	0.55
	Max.	7.57	6.27	5.71	-	5.03	5.71
	Min.	3.05	3.05	3.05	-	2.49	2.49

\*\*\* D<sub>n</sub> is the number average diameter of minor phase (μm)

Max. is the maximum drop size (μm)

Min. is the minimum drop size (μm)

All of these results can be explained in terms of the balancing between the viscous force ( $\gamma \eta_m$ ) and the interfacial tension force ( $\Gamma/R$ ). The ratio of viscous force and interfacial tension force is called "Capillary number (Ca)". At  $Ca \geq Ca_{crit}$ , the drop of minor phase is easy to break which generates smaller drop sizes (Wu, 1987). When the shear rate is increased, the viscous force, which is the force tends to elongate the drop which is proportional to shear rate, is higher than the interfacial tension force which is the force tends to keep the spherical shape. This imbalance between two forces provides the increase in Ca causing the elongation and breaking of the drops. The mechanism of drop deformation is shown in figure 4.12.

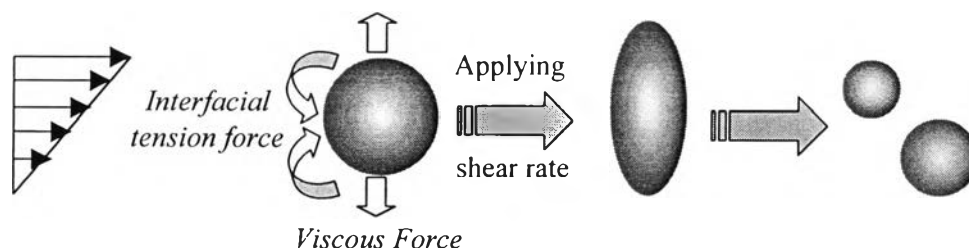


**Figure 4.12** The mechanism of drop deformation after applying the shear rate.

Moreover, the interfacial tension between the major and minor components is also an important parameter, which controls the drop size of minor phase as studied by Wu (1987). He gave a relation for the final droplet size of the minor phase as in equation 4.3:

$$D = \frac{4\Gamma\eta_r^{\pm 0.84}}{\gamma\eta_m} \quad (4.3)$$

where the plus (+) sign in the component applied for  $\eta_r > 1$  and the minus (-) sign in the component applied for  $\eta_r < 1$ . The drop sizes are generally smaller with diminution of the interfacial tension. The interfacial tensions between the PI minor phase and the matrices are shown in Table 4.5. The value of HDPE5200B/PI exhibits the highest whereas the lowest value belongs to the PS680A/PI blend. This is the reason why the drop size at any shear rates of HDPE5200B/PI and PS680A/PI are the largest and the smallest size, respectively.

**Table 4.5** The interfacial tension between PI minor phase and matrix at 220°C

Polymer Blends	$\Gamma$ (dyn/cm) <sup>*</sup>	$\Gamma$ (dyn/cm) <sup>#</sup>
HDPE5200B/PI	10.80	10.33 ± 1.78
PS680A/PI	4.48	5.08 ± 0.47
PVAc500/PI	8.31	7.73 ± 1.40

\* From calculation (Appendix C)

# From experiments (Appendix C)

From the plot between  $\log(D_n)$  versus  $\log(\text{shear rate})$  as shown in figure 4.10, the slopes of HDPE/PI, PS/PI and PVAc/PI are -1.12, -0.90 and -0.83, respectively. These results are consistent with Wu's correlation (1987) and Taylor's theory (1937) as shown in equations 4.3 and 4.4, respectively, that the slope of this plot should be close to -1.

$$D = \frac{4\Gamma(\eta_d + \eta_m)}{\gamma\eta_m\left(\frac{19}{4}\eta_d + 4\eta_m\right)} \quad (4.4)$$

The slope of PVAc/PI is quite different from the other two pairs because of its viscosity ratio ( $\eta_r$ ). The best range of  $\eta_r$  for breakup is between 0.5 to 1.0 (Folkes and Hope, 1993). For the HDPE/PI and PS/PI blends, the average  $\eta_r$  between the shear rate of 10 to 200  $\text{s}^{-1}$  are approximately 0.55 whereas the value of PVAc/PI blend is typically about 0.30. So PI minor phase of the PVAc/PI blend is more difficult to break.

To check that the steady state drop sizes producing during blending are from breakup or coalescence behaviors can be measured by the quantitative comparison of the steady state drop sizes from the experiments and the calculation by using Wu correlation as shown in equation 4.3. The results are tabulated in Table 4.6. If the coalescence behavior is important, it will give

sizes larger than those calculated by Wu but the breakup behavior will be more efficiency if the drop sizes give the similar values. By overall, it can be summarized that there is only breakup behavior occurs during the process because the  $D_n$  from the experiment and the calculation are close to each other at any shear rates.

**Table 4.6** The drop sizes of the three blends at any shear rates comparing between  $D_n$  from the experiment and the calculation

<b>Polymer Blends</b>	$\Gamma$ (dyn/cm)	$\gamma$ (s <sup>-1</sup> )	$\eta_m$ (Poise)	$\eta_r$	$D_n^*$ ( $\mu\text{m}$ )	$D_n^{**}$ ( $\mu\text{m}$ )
<b>PS/PI</b>	5.08	10	5,935	0.63	4.69 $\pm$ 0.52	5.05
		25	3,178	1.45	4.25	3.49
		100	1,305	0.48	3.68 $\pm$ 0.49	2.88
<b>HDPE/PI</b>	10.33	10	11,280	0.78	5.60 $\pm$ 0.75	5.48
		25	5,950	0.61	5.40	5.30
		100	1,643	0.40	4.62 $\pm$ 0.47	5.43
<b>PVAc/PI</b>	7.73	10	15,125	0.64	4.83 $\pm$ 0.66	4.25
		25	6,426	0.57	4.30	3.87
		100	2,433	0.27	3.93 $\pm$ 0.64	3.82

\* from the experiment (Table 4.4)

\*\* from the calculation (Equation 4.3)

#### 4.4.2) The Steady State Drop Size Distribution on Morphology

The droplet size distribution is a factor to check the equilibrium morphology of the blends. The plots of the size distribution function versus the drop size at various shear rates are shown in figure 4.13a to 4.13c. At the low shear rate of  $10\text{ s}^{-1}$ , the distribution of three polymer blends shift to a larger size with wider distribution and at higher shear rates the curve shifts to the smaller size with narrower distribution (Appendix D).

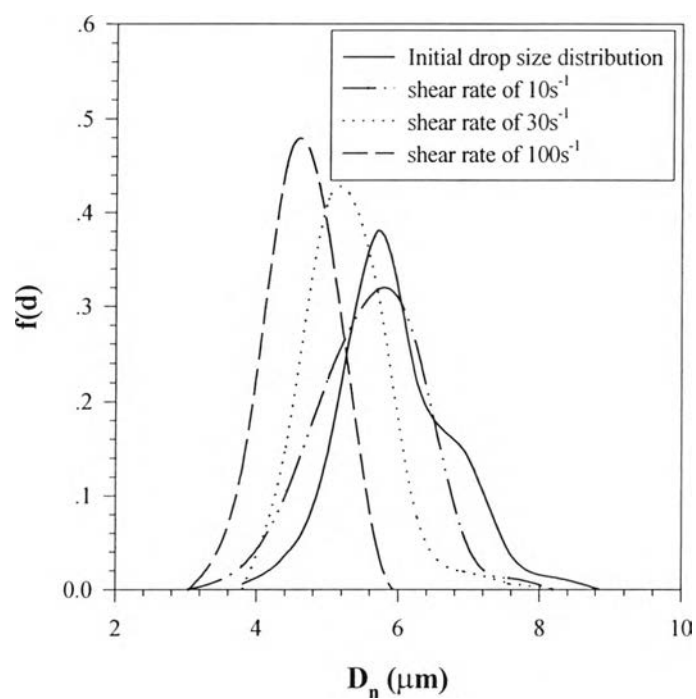


**Figure 4.13a** The drop size distribution of HDPE5200B/PI blend at various shear rates and at  $220^{\circ}\text{C}$ .

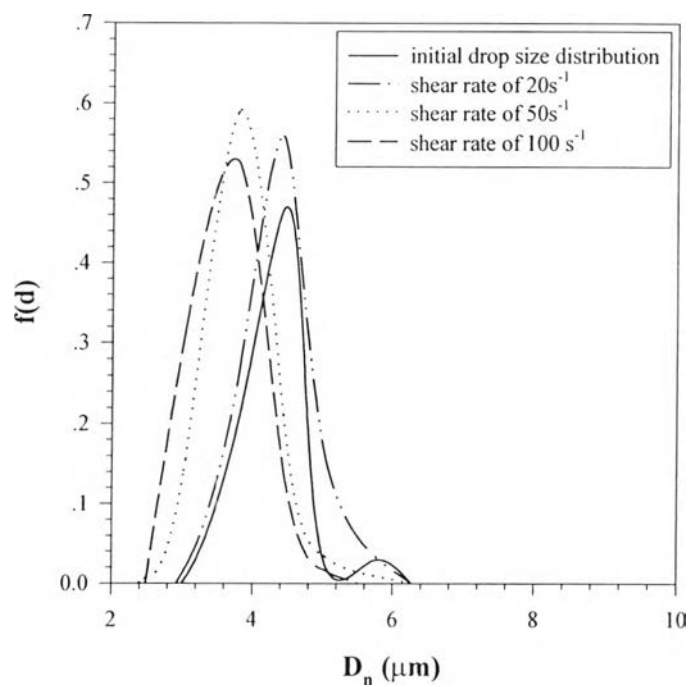


**Figure 4.13b** The drop size distribution of PS680A/PI blend at various shear rates and at 220°C.

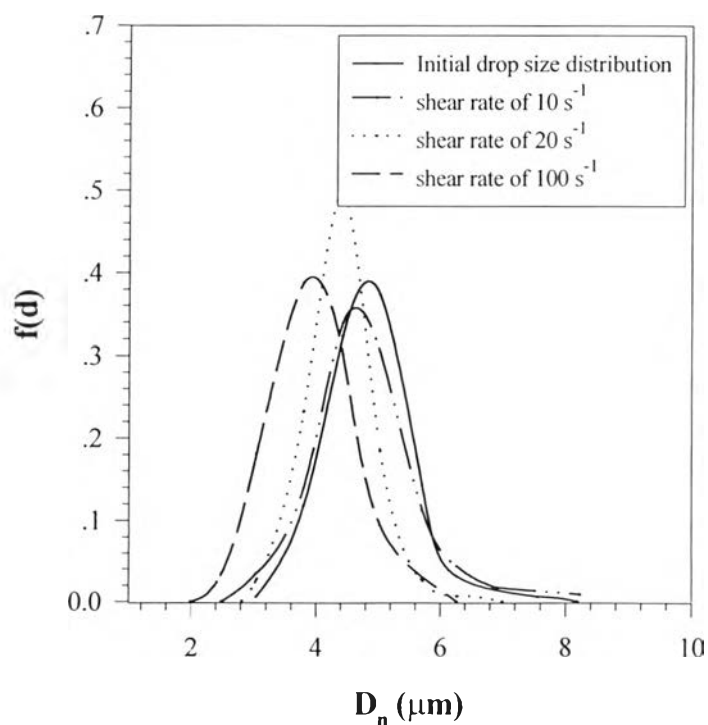


**Figure 4.13c** The drop size distribution of PVAc500/PI blend at various shear rates and at 220°C.

## 4.5 Effect of Triblock Copolymer on the Morphology

Triblock copolymer is one of compatibilizers used in controlling blend morphology. There are several published results (Jamieson *et al.*, 1996 and 1997, Sundararaj and Macosko, 1995). In this work, the effects of triblock copolymer on blend morphology as processed by the solvent casting process and the melt mixing process were investigated as a function of triblock copolymer concentration and shear rate.

### 4.5.1 Effect of Triblock Copolymer on the Solvent Casting Blends

As the poly(styrene-*b*-isoprene-*b*-styrene) triblock copolymer was added in the PS/PI blend by using chloroform as a solvent, the block copolymer diffuses to the interface, decreases the interfacial tension between major and minor components and stabilizes the morphology against coalescence as shown in figure 4.14, leading to a decrease in droplet size.

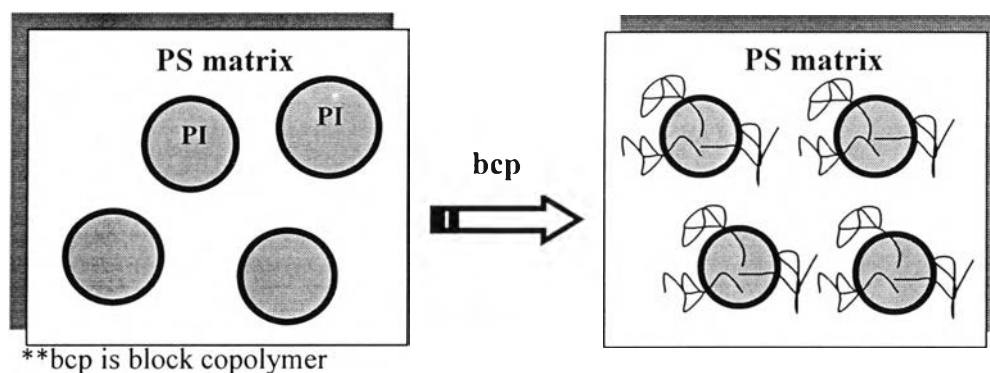


**Figure 4.14** Schematic of droplet size of PS/PI blends as a function of block copolymer. Chloroform was used as the solvent.

The droplet sizes of the PS/PI blend decrease with increasing the triblock copolymer concentration. The droplet size is the smallest at 20% triblock copolymer whereas the largest size is obtained in the blends without block copolymer. This result is shown in figure 4.15.



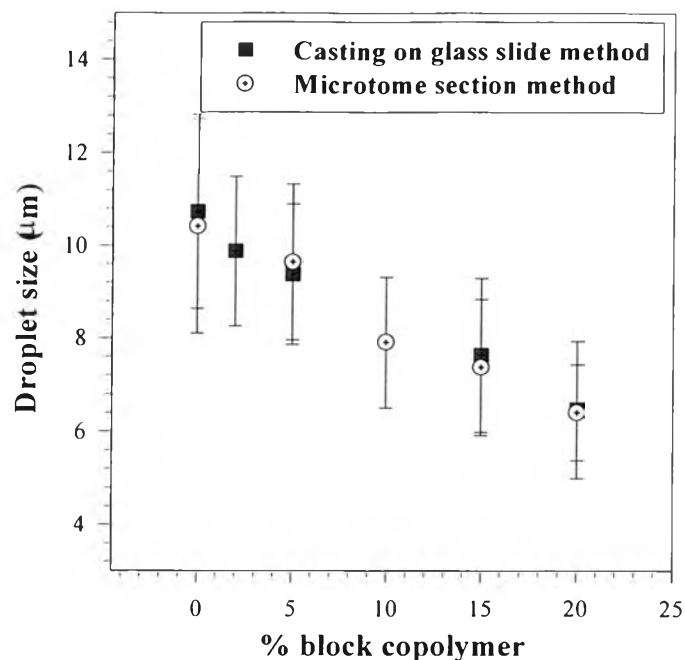


**Figure 4.15** Comparison the droplet sizes of PS/PI blend from the casting solution on glass slide and the microtome section method. Chloroform is acted as the solvent.

The drop sizes between the 2 methods: a) Casting solution on glass slide method and b) microtome section method are close to each other at the same concentration of triblock copolymer. The data of drop size and standard deviations (S.D.) of both methods are tabulated in Table 4.7. The differences in the drop sizes between the two methods are less than 5%.

These two methods have both advantages and disadvantages. In general, the microtome section method is more favorable to prepare a thin film because of the ability to control the film thickness. But it needs a long time to prepare a thick sample before cutting. For the casting solution on glass slide method, its advantage is the shorter time to prepare thin film whereas the difficulty to control the film thickness is its disadvantage.

**Table 4.7** The droplet size of PS/PI blend with 0 to 20% triblock copolymer of solvent casting process

% block copolymer	Droplet size (micrometers)	
	Casting on glass slide method	Microtome method
0	10.74 ± 2.08	10.42 ± 2.29
2	9.89 ± 1.60	-
5	9.39 ± 1.51	9.66 ± 1.66
10	-	7.91 ± 1.40
15	7.64 ± 1.65	7.38 ± 1.45
20	6.47 ± 1.46	6.42 ± 1.02

The size distribution was determined in order to investigate the morphology change with block copolymer concentration from 0, 2, 5, 10, 15 and 20%. These droplet size distributions as a function of triblock copolymer concentration are shown in figure 4.16 and figure 4.17, by plotting between droplet size (micrometers) versus  $f(d)$ . The size distributions exhibit very broad distribution at low percent of triblock copolymer and shift to narrower distributions at higher concentrations of block copolymer.

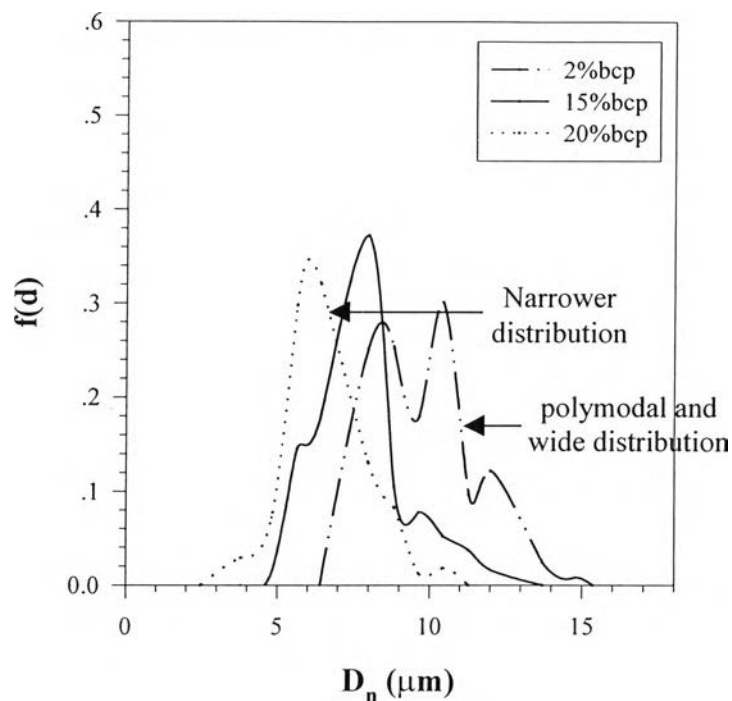


**Figure 4.16** Distribution function of droplet size for PS/PI blend at 0 to 20% SIS triblock copolymer (*Casting solution on glass slide method*).

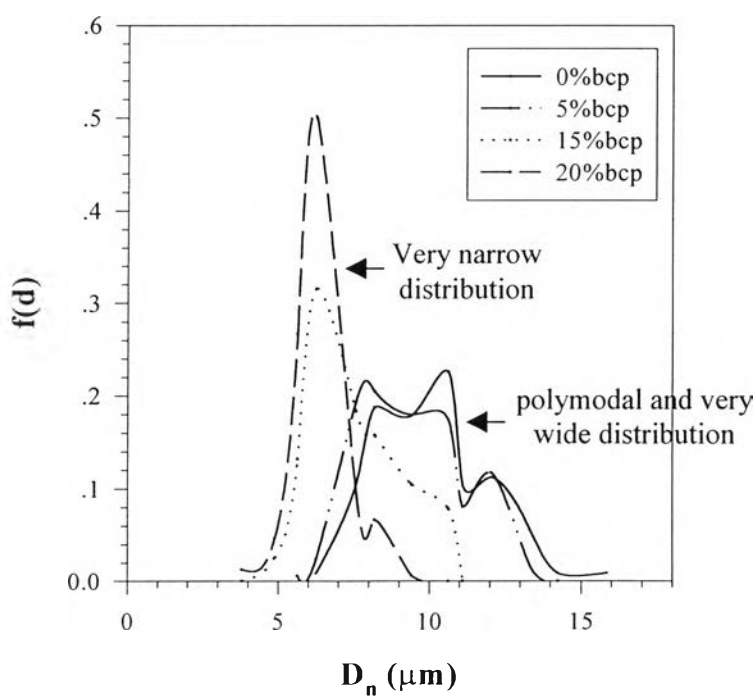


**Figure 4.17** Distribution function of droplet size for PS/PI blend at 0 to 20% SIS triblock copolymer (*Microtome section method*).

#### 4.5.2 Effect of Triblock Copolymer on the Melt Mixing Blends.

The effect of triblock copolymer on equilibrium drop size of melt mixing blends was investigated as a function of triblock copolymer concentration and shear rate. In this part, the polymer blends were mixed at  $10 \text{ s}^{-1}$  and at  $220^\circ\text{C}$ .

##### a) The Effect of Triblock Copolymer Concentration.

The drop sizes as a function of triblock copolymer concentration of three polymer blends are shown in figure 4.18 by plotting between the number average diameter of the PI minor phase versus the concentration of triblock copolymer. Increase in block copolymer concentration results in more block copolymer molecules available at the interface, leading to an increase in interfacial area, which means that a finer morphology is produced and the saturated drop size is obtained at higher concentrations. 2% triblock copolymer is the minimum concentration required to saturate the surface of the PI minor phase in all the blends studied.

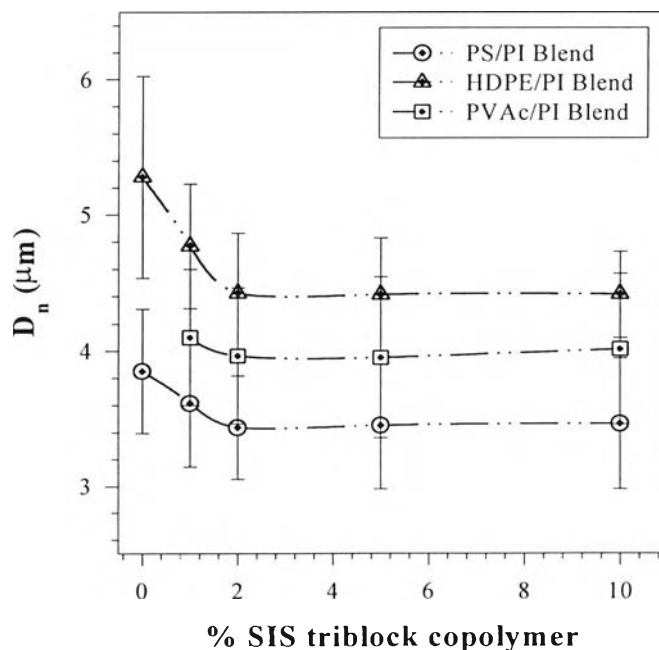


**Figure 4.18** The plot between  $D_n$  versus % triblock copolymer of three polymer blends at  $220^\circ\text{C}$  by mixing at  $10 \text{ s}^{-1}$  and shearing at  $50 \text{ s}^{-1}$ .

The droplet size generally decreases with increasing the shear rate (figure 4.11) generating the higher surface area of the drops. So the saturated concentration of the triblock copolymer for shearing at higher shear rates should be more than that of lower shear rate. The plot between  $D_n$  versus % triblock copolymer of HDPE/PI blend by shearing at  $100\text{ s}^{-1}$ ,  $220^\circ\text{C}$  is shown in figure 4.19. The plot shows that the saturated triblock copolymer concentration changes from 2% to be approximately 5% when the shearing rates adjusts from  $50\text{ s}^{-1}$  to  $100\text{ s}^{-1}$  and  $D_n$  value are independent of the triblock copolymer concentration when it is above 5%.

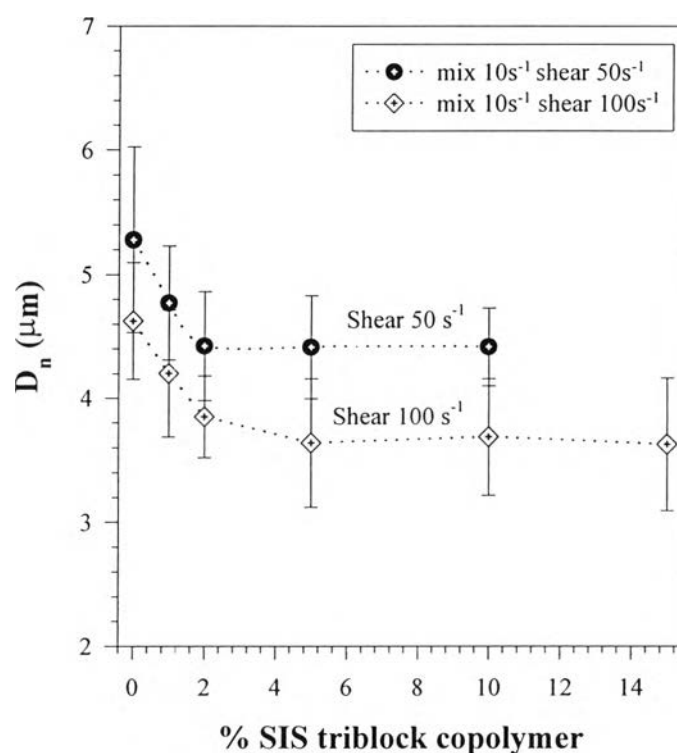


**Figure 4.19** The plot between  $D_n$  versus triblock copolymer concentration of HDPE/PI blend at the shear rates of 50 and  $100\text{ s}^{-1}$ ,  $220^\circ\text{C}$ .

b) The Saturated Drop Size as a Function of Shear Rate

1. Step-Up of Shear Rate: Breakup Experiment

The drop sizes as a function of shear rate of three polymer blends with 5% SIS triblock copolymer were investigated and shown in figure 4.20a to figure 4.20c. The drop size decreases with increasing the shear rate with both 0 and 5% triblock copolymer but  $D_n$  at 5% triblock copolymer is smaller than that of 0% triblock copolymer at any shear rates. At 5% block copolymer, the drop size reductions in the HDPE/PI and PS/PI blends are the greatest (~12-14%) relative to the blends with 0%block copolymer whereas the drop size reduction of the PVAc/PI blend is only 2-5 %.

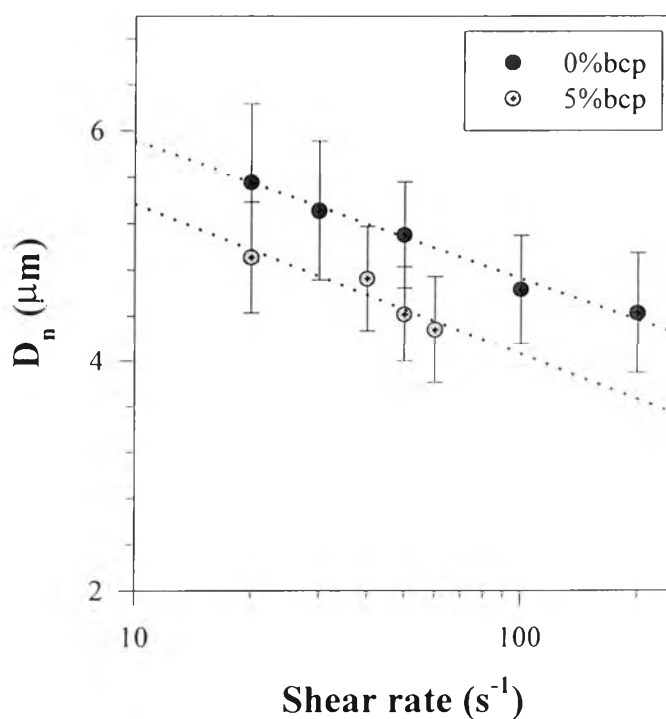


**Figure 4.20a** The plot between drop size ( $D_n$ ) versus shear rates of the HDPE/PI blend at 220°C comparing between 0 and 5 % SIS triblock copolymer.

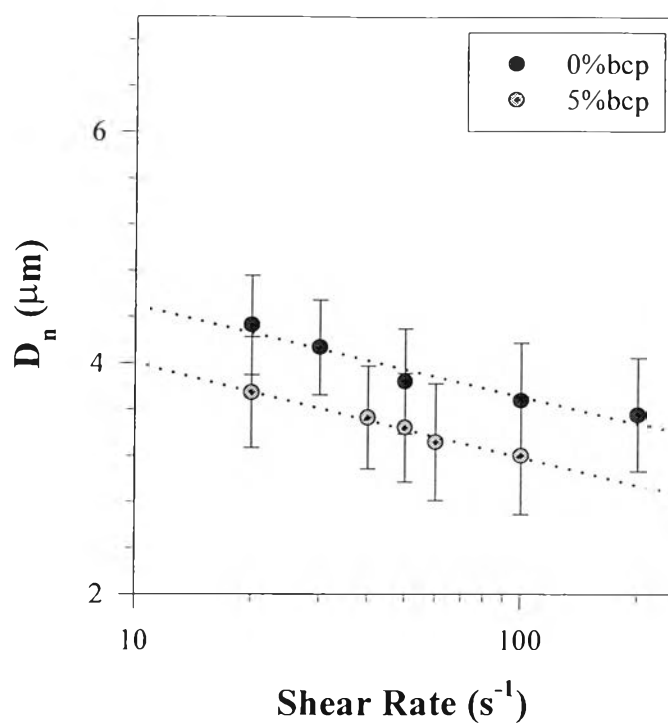


**Figure 4.20b** The plot between drop size ( $D_n$ ) versus shear rates of the PS/PI blend at 220°C comparing between 0 and 5 %SIS triblock copolymer.

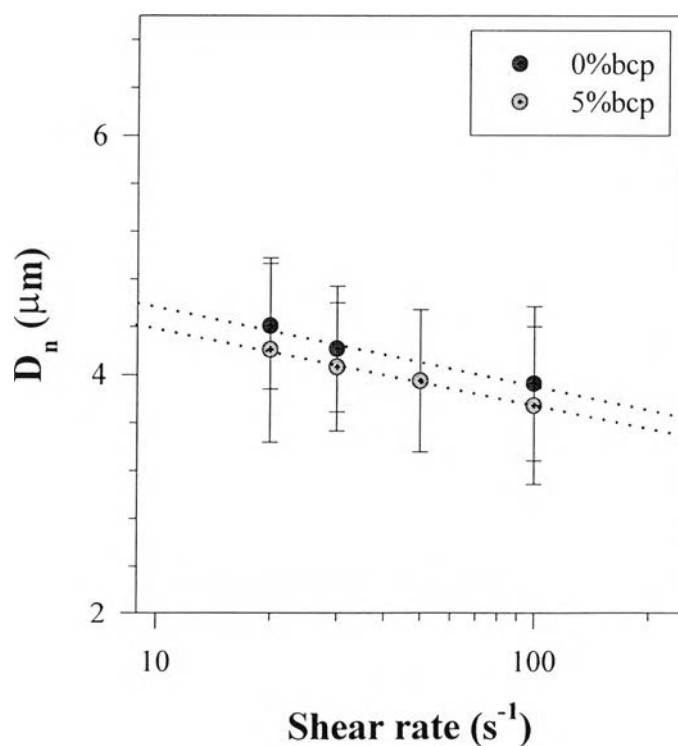


**Figure 4.20c** Plot between drop size ( $D_n$ ) versus shear rates of the PVAc/PI blend at 220°C comparing between 0 and 5 %SIS triblock copolymer.

The reduction of drop size at 5% triblock copolymer occurs because of the swelling between polymer and its compatible segment of block copolymer. From the swelling equation,

$$\text{Swelling}(S) = -2\chi N + \frac{N}{P} \quad (4.5)$$

where N and P are degrees of polymerization of block copolymer segment and homopolymer, respectively. Generally, two types of swelling are formed in the polymer blends with block copolymer system. They are a) the swelling between minor phase (PI) and its compatible segment (PI segment of block copolymer) which is called “ $S_{in}$ ” and b) the swelling between major component and its compatible segment (PS segment of block copolymer) which is called “ $S_{out}$ ” (Jamieson *et al.*, 1998). In this work,  $S_{in}$  is always constant in every system whereas  $S_{out}$  is varied. Parameters used in calculating swelling and the values of swelling in each blend are tabulated in Tables 4.8 and 4.9, respectively.

**Table 4.8**  $\bar{M}_n$ ,  $M_0$ , N and P of each polymer used in blending

Polymer	$\bar{M}_n$ (g/mole)*	$M_0$	$N^{\#}$	$P^{\#}$
PS680A	57,173	104	-	549.74
HDPE5200B	50,185	28	-	1792.32
PVAc500	79,100	86	-	919.77
PI	64,709	68	-	951.60
PI segment	22,410	68	329.56	-
PS segment	52,290	104	502.79	-

\* from experiment (GPC and rheometer)

# from calculation

$M_0$  is the molecular weight of a repeating unit



**Table 4.9** The swelling ( $S_{in}$  and  $S_{out}$ ) and the swelling ratio of three polymer blends

Polymer blends	Swelling (S)*		Swelling Ratio
	$S_{in}$	$S_{out}$	
HDPE / PS-b-PI / PI	0.346	-14.20	-41.04
PS / PS-b-PI / PI	0.346	0.91	2.63
PVAc / PS-b-PI / PI	0.346	-25.90	-74.85

\* from calculation (equation 4.5)

Generally, strongly swollen PS segments of the block copolymer on the outer part of the interface ( $S_{out}$ ), make the interface more immobile which provides a lower probability of coalescence by increasing the friction at the interface when the fluid film between two droplets drains (Jamieson *et al.*, 1997). That is why the drop size of PS/PI blend decreases more rapidly than the other two blends. Because there is only the breakup behavior occurs during the process, the interfacial tension is the parameter in controlling the drop size. The droplet sizes of the PS/PI blend are the smallest because of the lowest interfacial tension whereas the largest size belongs to the HDPE/PI blend.

### 2) Step-Down of Shear Rates: Coalescence Experiment

Generally, block copolymer has a greater influence in the coalescence behavior than the breakup behavior (Miles and Rostami, 1992). To study the effect of triblock copolymer on coalescence, we need to step down from a high shear rate to a low shear rate and the results are tabulated in Table 4.10. The blends were mixed at  $100 \text{ s}^{-1}$  and followed by shearing at a lower shear rate of  $10 \text{ s}^{-1}$  to induce coalescence.

**Table 4.10**  $D_n$  of three blends at 0 and 5% SIS triblock copolymer comparing between the size of mixing at  $100 \text{ s}^{-1}$  and that of shearing at  $10 \text{ s}^{-1}$ ,  $220^\circ\text{C}$ . The strain unit was fixed at 6,000 in all the blends studied

Polymer Blends	Drop size ( $\mu\text{m}$ )				% changing *	
	Mixing at $100 \text{ s}^{-1}$		Shearing at $10 \text{ s}^{-1}$		0% bcp	5% bcp
	0% bcp	5% bcp	0% bcp	5% bcp		
HDPE/PI	$4.53 \pm 0.71$	$4.37 \pm 0.56$	$5.01 \pm 0.78$	$4.56 \pm 0.61$	9.58	4.17
PS/PI	$4.05 \pm 0.57$	$3.98 \pm 0.44$	$4.28 \pm 0.56$	$4.02 \pm 0.49$	5.37	0.99
PVAc/PI	$4.44 \pm 0.57$	$4.18 \pm 0.66$	$5.03 \pm 0.71$	$4.43 \pm 0.68$	11.73	5.64

\* % changing is the drop size ratio between mixing at  $100 \text{ s}^{-1}$  and shearing at  $10 \text{ s}^{-1}$ .

During the mixing, the blends attained the equilibrium morphology by using the strain unit of 6000 and the drop size with 5% SIS triblock copolymer are smaller than that of 0% SIS triblock copolymer. This is because of higher steric hindrance and swelling effect between PS segment of block copolymer and matrix. At higher swelling, the steric hindrance between two drops increases providing the decrease in both  $P_{\text{coll}}$  and  $P_{\text{drain}}$ . So the coalescence in the system having high swelling is generally low. As shown in Table 4.8, the swelling of PS/PI blend has the highest value whereas that of the PVAc/PI blend has the lowest. So that is why the drop sizes of the PS/PI and the PVAc/PI blends increase at the lowest and highest rates, respectively.

The results after shearing at lower shear rate of  $10 \text{ s}^{-1}$  are also consistent with the previous one and breakup experiment. The interesting point is the comparison between the data of the blends at 0 and 5% SIS triblock copolymer after mixing at  $100 \text{ s}^{-1}$  and shearing at  $10 \text{ s}^{-1}$ . It shows that the drop sizes of all blends after shearing at lower shear rates are larger in the different ratio because of coalescence behavior as tabulated in Table 4.9. Generally, coalescence probability ( $P_{\text{coal}}$ ) depends on 2 parameters: collision probability ( $P_{\text{coll}}$ ) and film drainage probability ( $P_{\text{drain}}$ ). At lower shear rates, both  $P_{\text{coll}}$  and  $P_{\text{drain}}$  are higher leading to increasing of  $P_{\text{coal}}$ .

$$P_{\text{coal}} = P_{\text{coll}} \cdot P_{\text{drain}} \quad (4.6)$$

The plot between diameter ratio, the ratio between  $D_n$  after shearing at  $10 \text{ s}^{-1}$  divided by  $D_n$  after mixing at  $100 \text{ s}^{-1}$ , versus swelling ratio are shown in figure 4.21. It indicates that higher swelling ratio leads to a higher efficiency in preventing coalescence. So this is the reason why the diameter ratio of the PS/PI blend exhibits the lowest value whereas the highest ratio belongs to the PVAc/PI blend.

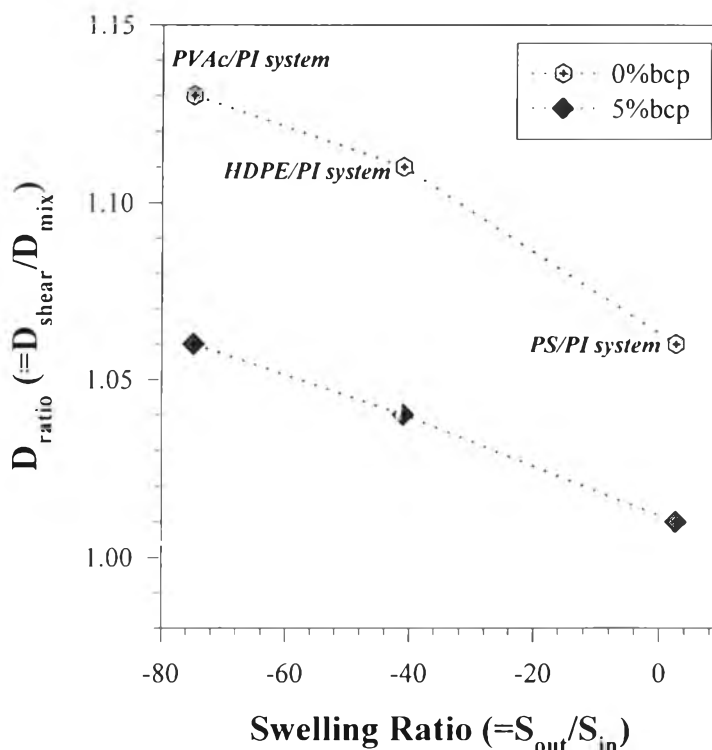


**Figure 4.21** The plot between diameter ratio versus swelling ratio of three blends with 0 and 5% SIS triblock copolymer and at  $220^\circ\text{C}$ .

The drop size distribution function is also an important parameter for studying the effect of block copolymer on coalescence behavior. The results of these three blends at 0 and 5% SIS triblock copolymer after mixing at  $100 \text{ s}^{-1}$  and shearing at lower shear rate of  $10 \text{ s}^{-1}$  are shown in figure 4.22a to 4.22c. In all blends show the drop size distribution shifts to the lower size when block

copolymer was added and distribution of lower shear rates shifts to the larger size than that of the higher shear rate. This is because of the formation of the drop size.

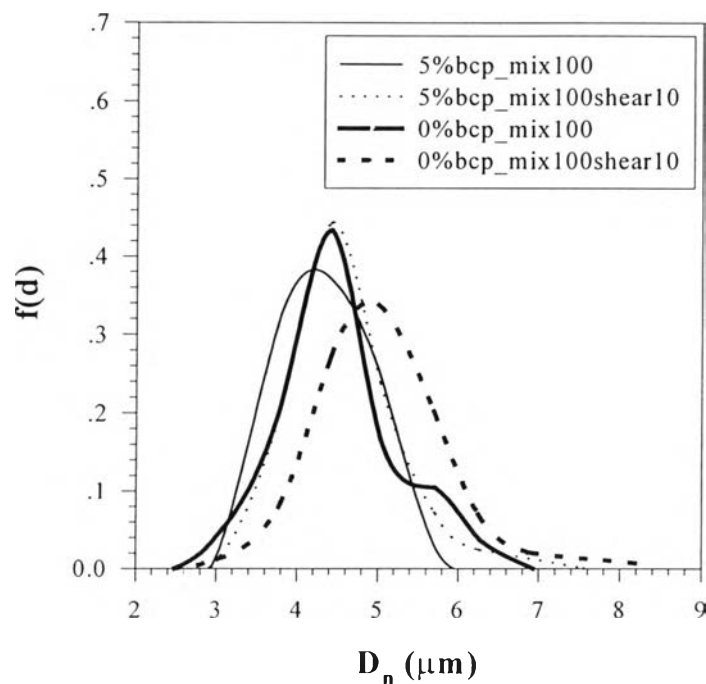


**Figure 4.22a** The drop size distribution of HDPE/PI with 0 and 5% SIS triblock copolymer after mixing and shearing at 100 and  $10 \text{ s}^{-1}$ , respectively.

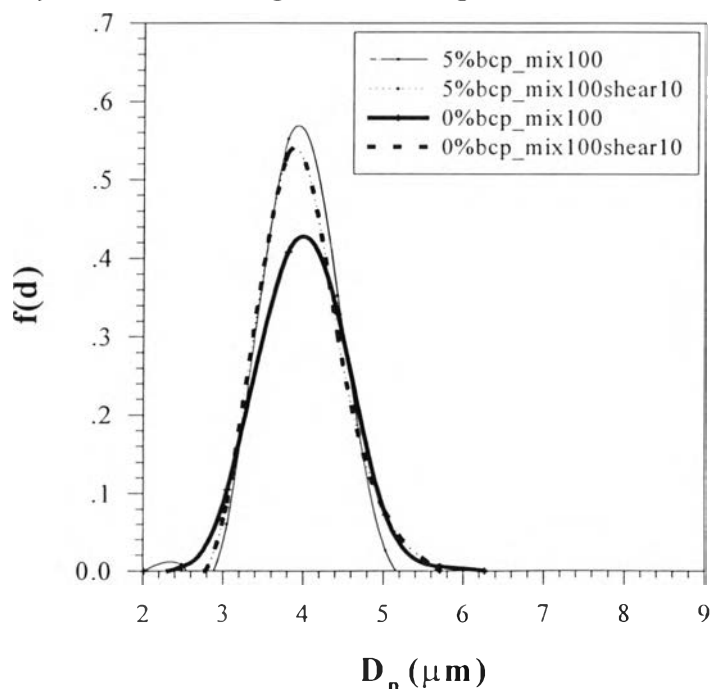


**Figure 4.22b** The drop size distribution of PS/PI with 0 and 5% SIS triblock copolymer after mixing and shearing at 100 and  $10 \text{ s}^{-1}$ , respectively.

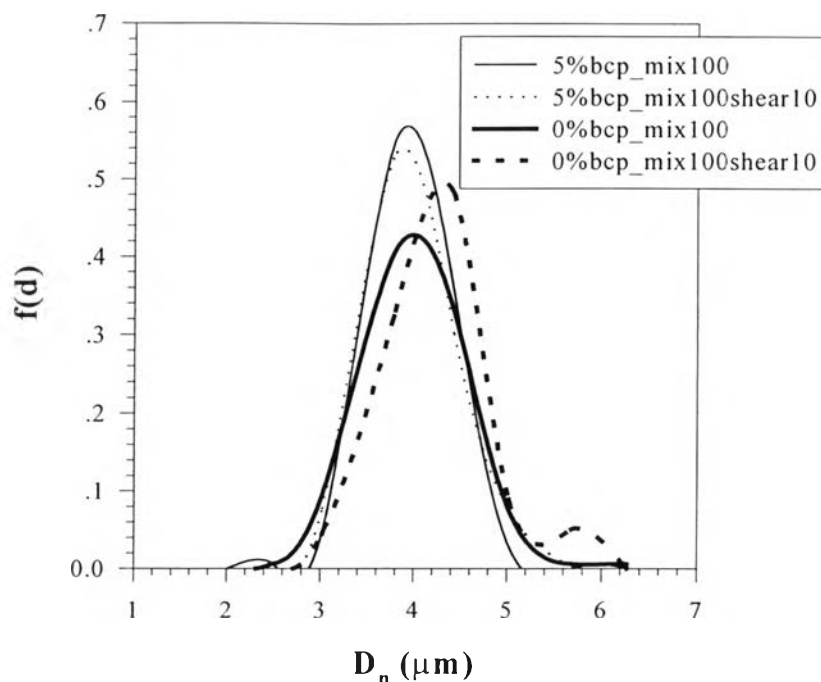
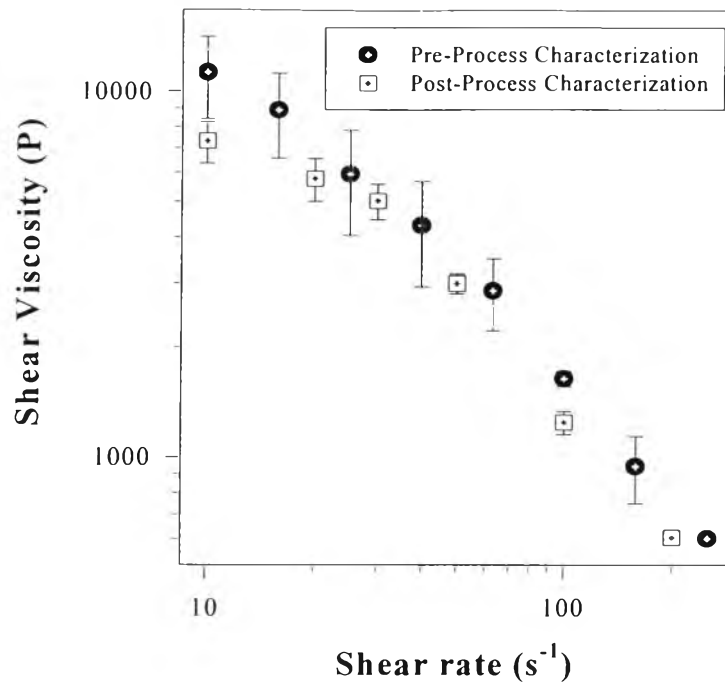


**Figure 4.22c** The drop size distribution of PVAc/PI with 0 and 5% SIS triblock copolymer after mixing and shearing at 100 and 10  $s^{-1}$ , respectively.

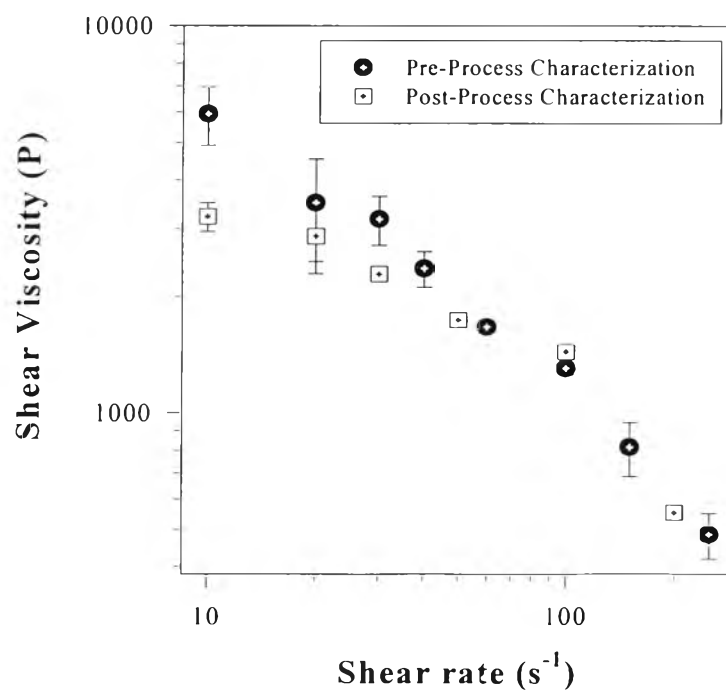
#### 4.6 Post-Process Characterization of Homopolymers

Shearing temperature, shearing rate, time, heating and so on are important parameters leading to polymer degradation during process. Post process characterization of each polymer is one method to check the polymer degradation. The results of shear viscosity and  $N_1$  of each polymer comparing between pre-process and post-process are shown in figure 4.23 and 4.24, respectively.

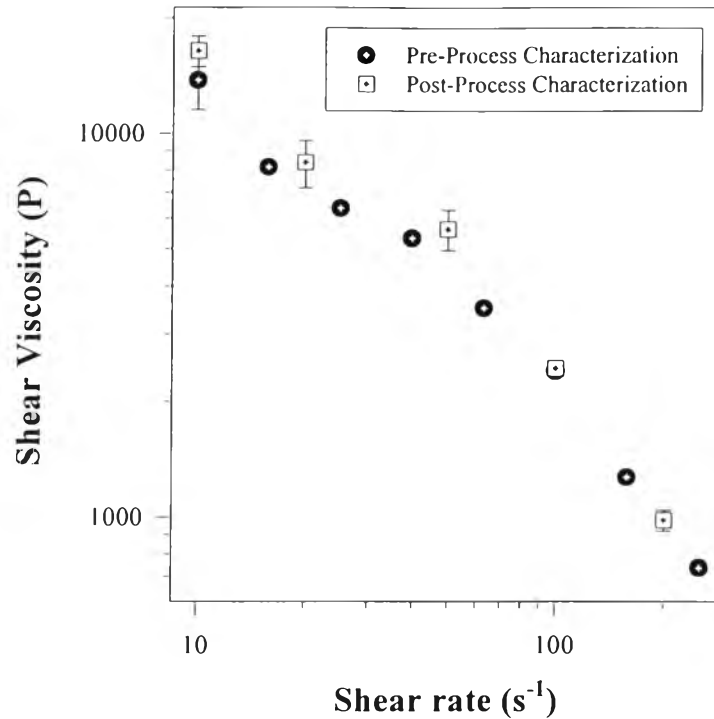
For the shear viscosity measurement of HDPE5200B, the polymer degradation occurred at low shear rates between 10 to 20  $s^{-1}$  because the value changed more than 10% whereas no degradation occurred at higher shear rates. PS680A showed the similar result with HDPE but the polymer degradation was generated at the shear rate of 10 to 30  $s^{-1}$ . PVAc500 was only one material that did not degrade between the shear rates of 10 to 200  $s^{-1}$ .



**Figure 4.23a** The shear viscosity of HDPE5200B at 220°C comparing between before process and after process. The strain unit of 6000 was used in the process.

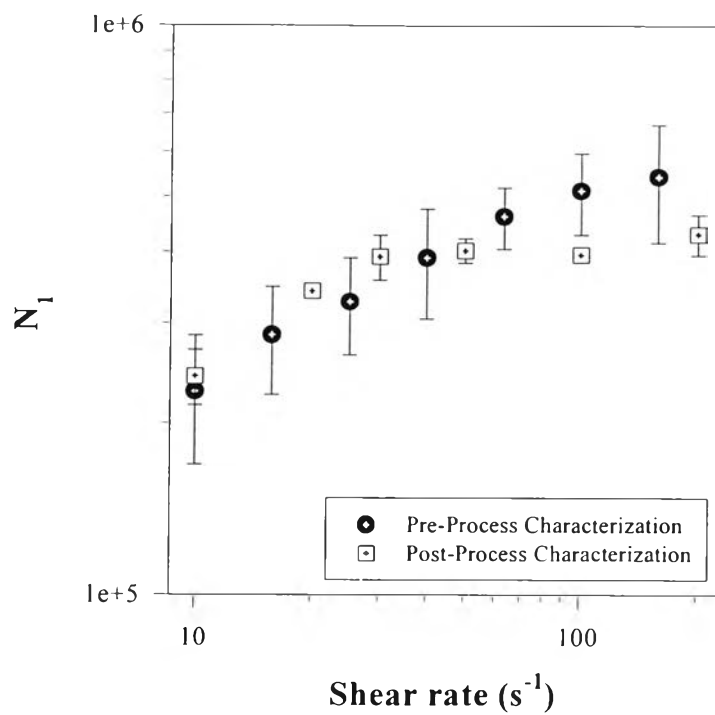


**Figure 4.23b** The shear viscosity of PS680A at 220°C comparing between before process and after process.

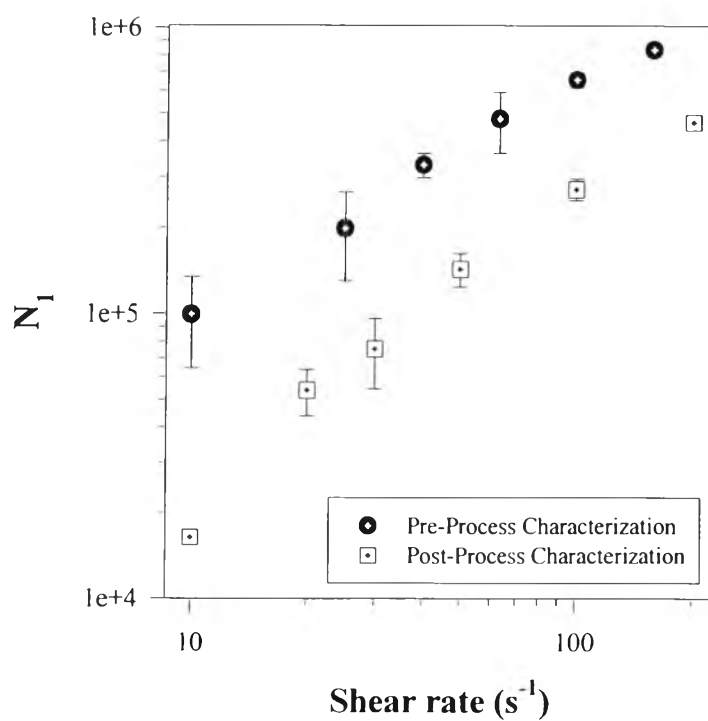


**Figure 4.23c** The shear viscosity of PVAc500 at 220°C comparing between before process and after process.

The first normal stress difference of each polymer is also important to measure after processing. The results are shown in figure 4.24a to 4.24c.  $N_1$  for the three polymers changed more than that of shear viscosity. This was because the shear viscosity depends on  $M_w^{3.4}$  (Mark, Bikales, Overberger and Menges, 1985) whereas  $N_1$  depends on  $M_w^7$  (Morrison, 1999). When a polymer degrades, its molecular weight is changed. That was the reason why the changing of  $N_1$  was faster than that of the shear viscosity. PVAc500 was still only one material that had the same  $N_1$  between before and after process.  $N_1$  of HDPE5200B started to change dramatically after the shear rate of  $50 \text{ s}^{-1}$  whereas that of PS680A was changed most rapidly along the range of shear rates.

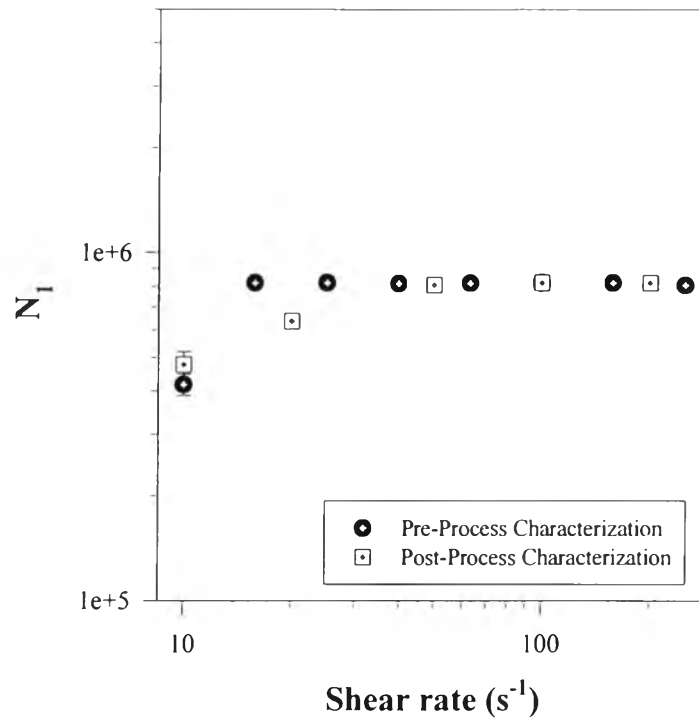


**Figure 4.24a**  $N_1$  of HDPE5200B at 220°C comparing between before process and after process. The strain unit of 6000 was used in the process.



**Figure 4.24b**  $N_1$  of PS680A at 220°C comparing between before process and after process. The strain unit of 6000 was used in the process.

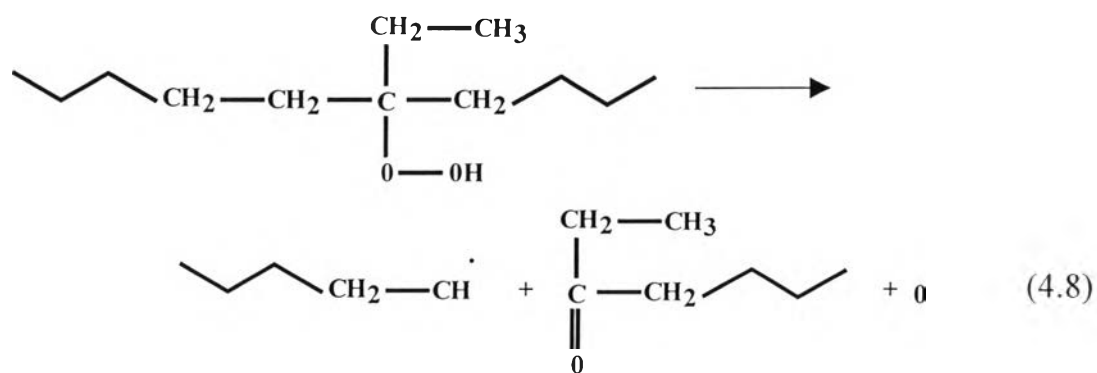
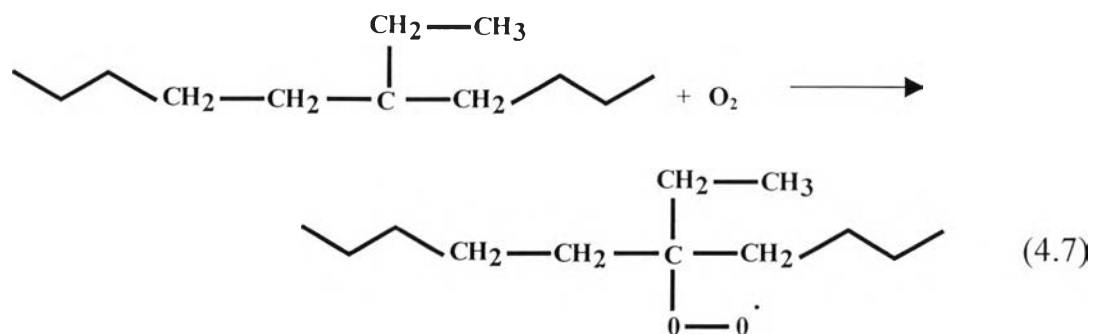




**Figure 4.24c**  $N_1$  of PVAc500 at 220°C comparing between before process and after process. The strain unit of 6000 was used in the process.

Almost polymers especially PE and PP are sensitive to oxidize that occurs on exposure to strong oxidizing agents or even in air under ultraviolet light as well as elevated temperatures during processing or service life (Dorel and Alla, 1996). So the degradation of all polymers used in this work occurred because of the oxidation reaction during shearing at high temperature in the atmosphere. The oxidation proceeds by a free radical mechanism through the formation of hydroperoxides which decomposes to new free radicals and the reaction is autocatalytic (Dorel and Alla, 1996) as shown in equations 4.7 and 4.8. Two kinds of reactions can take place on oxidation:

- (a) the scission of polymer chains that leads to a deterioration of the mechanical properties as a result of the reduction of the MW:



(b) At higher levels of oxidation, combination reactions between existing radicals result in crosslinking of polymer chains and the formation of brittle products.